A Distributionally Robust Co-Ordinated Reserve Scheduling Model Considering CVaR-Based Wind Power Reserve Requirements

Zhen Wang, *Member, IEEE*, Qiaoyan Bian, *Student Member, IEEE*, Huanhai Xin, *Member, IEEE*, and Deqiang Gan, *Senior Member, IEEE*

***Abstract*—The reserve scheduling problem becomes more difficult to handle when wind power is increasing at a rapid rate in power systems and the complete information on the stochasticity of wind power is hard to be obtained. In this paper, considering the uncertainty on the probability distribution (PD) of the wind power forecast error (WPFE), a distributionally robust co-ordinated reserve scheduling (DRCRS) model is proposed, aiming to minimize the total procurement cost of conventional generation and reserve, while satisfying the security requirement over all possible PDs of WPFE. In this model, a distributionally robust formulation based on the concept of conditional value-at-risk (CVaR) is presented to obtain the reserve requirement of wind power. In addition, to achieve tractability of the scheduling model, the random variable that refers to WPFE in the scheduling model is eliminated, equivalently converting the stochastic model into a deterministic bilinear matrix inequality problem that can be effectively solved. Case studies based on the IEEE-39 bus system are used to verify the effectiveness of the proposed method. The results are compared with the normal distribution based co-ordinated reserve scheduling (NDCRS) method that assumes WPFE is of normal distribution.**

***Index Terms*—Reserve schedule, wind power forecast error, probability distribution, conditional value-at-risk.**

NOMENCLATURE

Acronyms

WPFE	Wind power forecast error.
PD	Probability distribution.
DRCRS	Distributionally robust coordinated reserve scheduling.
NDCRS	Normal distribution coordinated reserve scheduling.
CVaR	Conditional value-at-risk.
VaR	Value-at-risk.
LMI	Linear matrix inequality.
BMI	Bilinear matrix inequality.

Parameters

R^n	n-dimension real space.
α	Risk level of wind power reserve insufficient.
$t, \Delta T$	Time period and time interval.
$\boldsymbol{\mu},\ \boldsymbol{\Gamma}$	Mean vector and covariance matrix of WPFE.
$\Phi(\boldsymbol{\mu}, \boldsymbol{\Gamma})$	Set of the PDs that have common $(\boldsymbol{\mu},\ \boldsymbol{\Gamma})$.
Ω_{RP}, Ω_{RT}	Bus set of generators that can provide the rolling-plan reserve and the real-time reserve, respectively.
Ω_G	Full generator bus set with $\Omega_{RP} \subset \Omega_G$ and $\Omega_{RT} \subset \Omega_G$.
N_G	Number of generators in Ω_G.
N_{RP}, N_{RT}	Number of generators in Ω_{RP} and Ω_{RT} respectively.
$\Omega_D, \Omega_W, \Omega_L$	Set of loads, wind farms and transmission lines.
$\bar{r}_{Gi}^{up}/\bar{r}_{Gi}^{dn}$	The ith unit's limit value for the up/down ramping rate.
$a_{Gj}^{up,rt}/a_{Gj}^{dn,rt}$, $a_{Gk}^{up,rp}/a_{Gk}^{dn,rp}$	The procurement cost coefficients for the real-time reserve and the rolling-plan reserve, respectively. $j \in \Omega_{RT}$, $k \in \Omega_{RP}$.
T_5, T_{15}	Reserve execution cycle, $T_5 = 5\,\mathrm{min}$ and $T_{15} = 15\,\mathrm{min}$.
a_{1i}	Generation cost coefficient.
$\bar{P}_{Gi}/\underline{P}_{Gi}$	The ith unit's maximum/minimum power output.
$\bar{P}_{Ll}/\underline{P}_{Ll}$	The upper/lower limit of active power flow through the lth transmission line.
T	The network distribution factor matrix.
$\boldsymbol{C_G}, \boldsymbol{C_{RT}}, \boldsymbol{C_W}, \boldsymbol{C_D}$	Constant matrixes, their element (i, j) is 1 if the jth generator/real-time reserve/wind power/load is connected to bus i, and 0 otherwise.
$1-\beta$	Confidence level of security requirement.

Variables

$R_{C_\alpha,t}$	Wind power reserve capacity with risk level α at time period t.
$\boldsymbol{P_W}, \boldsymbol{P_W^f}$	Real and forecasted vector of wind power, respectively. $\boldsymbol{P_W}, \boldsymbol{P_W^f} \in \mathbb{R}^n$.

Manuscript received April 15, 2015; revised August 17, 2015 and October 18, 2015; accepted October 30, 2015. Date of publication December 03, 2015; date of current version March 18, 2016. This work was supported in part by the National Nature Science Foundation of China under Grants 51177146 and 51277160, and in part by the National High Technology Research and Development Program of China under Grant 2015AA050202. Paper no. TSTE-00291-2015.

Z. Wang, H. Xin, and D. Gan are with the Department of Electrical Engineering, Zhejiang University, Zhejiang 310027, China, and also with the Key Laboratory of Renewable Energy of Zhejiang Province, Zhejiang 310027, China (e-mail: xinhh@zju.edu.cn; eezwang@ieee.org).

Q. Bian is with Hangzhou Power Supply Company of State Grid Zhejiang Electric Power Company, Zhejiang 310009, China.

Color versions of one or more of the figures in this paper are available online at http://ieeexplore.ieee.org.

Digital Object Identifier 10.1109/TSTE.2015.2498202

$\boldsymbol{\xi}$	The random variable of WPFE, $\boldsymbol{\xi} = \boldsymbol{P_W} - \boldsymbol{P_W^f}$, $\boldsymbol{\xi} \in \mathbb{R}^n$.
$R(\boldsymbol{\xi})$	Reserve requirement caused by the WPFE variable $\boldsymbol{\xi}$.
$\phi(\boldsymbol{\xi})$	Probability density function of $\boldsymbol{\xi}$.
$\boldsymbol{P_{G,t}}$	Active power vector with element $P_{Gi,t}$, $i \in \Omega_G$.
$\lambda_{Gj,t}^{up,rt}/\lambda_{Gj,t}^{dn,rt}$	The up/down capacity procurement factor for the real-time reserve of the jth generator, $j \in \Omega_{RT}$.
$\lambda_{Gk,t}^{up,rp}/\lambda_{Gk,t}^{dn,rp}$	The procurement factor of the up/down rolling-plan reserve for the kth units, $k \in \Omega_{RP}$.
$\boldsymbol{d_{G,t}^{rt}}$	The distribution coefficient vector for the jth unit's real-time reserve with $\sum_{j\in\Omega_{RT}} d_{Gj,t}^{rt} = -1$.
$\boldsymbol{P_{D,t}}$	Power load vector with element $P_{Di,t}$, $i \in \Omega_D$.
$\boldsymbol{P_{L,t}^f}/\boldsymbol{P_{L,t}^{rt}}$	Power flow vector with the forecasted/real value $P_{Ll,t}^f/P_{Ll,t}^{rt}$, $l \in \Omega_L$ through the lth transmission line.
$\boldsymbol{P_t^f}/\boldsymbol{P_t^{rt}}$	The forecasted/real power injection vector.
R_L^{up}/R_L^{dn}	The total up/down reserve capacity requirement caused by load fluctuation.
R_W^{up}/R_W^{dn}	The total up/down reserve capacity requirement caused by wind power fluctuation or WPFE.
$R_{sys}^{up}/R_{sys}^{dn}$	The total up/down reserve capacity requirement caused by system contingency.
$R_{\min}^{up,rt}/R_{\min}^{dn,rt}$	The total up/down capacity requirement of the real-time reserve.
$R_{\min}^{up,rp}/R_{\min}^{dn,rp}$	The total up/down capacity requirement of the rolling-plan reserve.
$\boldsymbol{R_{G,t}^{rt}}$	The real-time reserve vector of the jth unit $R_{Gj,t}^{rt}$, $j \in \Omega_{RT}$.

I. Introduction

As THE penetration of wind power increases significantly in power systems, wind power variability and forecast uncertainty pose big challenges on power system planning and operation [1]. To mitigate the effect of uncertainties of wind power, system loads and contingency events on power grids, various reserves over different time-horizons need to be scheduled. Therefore, how to quantify the reserve requirements and allocate the reserves among the conventional generators becomes an essential problem in power systems.

The operational and economic impact of wind power uncertainty on the reserve scheduling has been investigated in many literatures. In [2], a reserve optimization model considering the wind power forecast error (WPFE) is proposed. The net demand error is assumed to be normal distribution and divided into several intervals and a cost/benefit analysis is carried out on each interval to calculate the optimal reserve requirements. A stochastic programming market-clearing model considering network constraints and costs of wind spillage is developed in [3] to find the optimal reserve levels and costs. A conditional value-at-risk (CVaR)-based reserve capacity decision method is proposed in [4], where a coordination and optimal reserve allocation model is formulated as well. The idea of wind power at risk in [5] is similar to that in [4], and the credibility theory is applied to estimate the operating reserve capacity. However, only a few literature have considered the ramping constraints of the conventional generation in [4] and [6], as well as the coordination of different reserves such as those in [4] and [7].

To cope with the uncertainty of wind power, the distribution of uncertainty variables is usually assumed to be known and given in advance. For example, WPFE is regarded as the random variable of normal distribution in [2], [7] and [8]. In [4], Laplace distribution is used to describe the WPFE variable. In [9], the wind power is assumed to comply with the Normal distribution, and the Latin Hypercube Sampling technique is applied to generate wind power scenarios. The Weibull distribution and Rayleigh distribution are used to describe the variation of wind speed in [10] and [11], and analytical tools including convolution and Fourier transform are employed to calculate the probability density function of wind power.

On the other hand, although the wind power forecasting techniques are developing rapidly in recent years, existing techniques mainly focus on forecasting the point values and the general information of WPFE, such as the expected value and the variance [12], which indicates that in reality only partial information about the probability distribution (PD) of WPFE can be obtained. Several literatures have been devoted to estimating the PD of WPFE. Normal distribution was early proposed and has gained wide-ranging applications such as in [8] and [13]. However, it is challenged in some works [14], [15]. Researchers propose beta distribution as an alternative in [14], [16] and [17], while it is pointed out that a heavy computation burden is needed to solve the beta distribution and infinite great probabilities may be obtained in some cases [15]. Other distributions such as the mixed Laplace distribution is used in [15] and [18], the Cauchy distribution is adopted in [19], and a Lévy α-stable distribution is proposed in [20]. However, due to the diversity of geographical locations, weather conditions and even forecasting tools, there is no such uniform PD that is suitable to describe the WPFE distribution in all different situations. Instead, the PD is uncertain and attributes to a special set of distributions with certain partial information, such as the first- and second-order moments, which can be collected from the historical data. Consequently, the above reserve scheduling methods may be ineffective in such circumstances, which motivates new methods to be developed to solve the reserve scheduling problem with wind power integration.

In our previous work [23], a distributionally robust optimization model considering a single time-scale reserve schedule is proposed. In this paper, a multiple time-scale reserves coordination model is developed to handle the de-facto various time-scale reserves. Further, some CVaR-based wind power reserve conditions are introduced to balance reliability and economy of reserve requirement. A distributionally robust coordinated reserve scheduling (DRCRS) model is presented, aiming to minimize the procurement cost of generation and different time-scale reserves. Meanwhile, in the model the embedded requirements over all possible PDs of WPFE with common statistic information, e.g., the first- and second-order moment is well satisfied. In this model, the wind power reserve are formulated based on the concept of CVaR. To achieve tractability of the DRCRS model, the formulation of CVaR-based wind power reserve capacity is converted into an LMI problem, and the S-lemma [21] and the Schur complements [22] are used to convert the probabilistic DRCRS model into an equivalent deterministic BMI constrained problem, which can be solved by existing optimization methods.

The rest of this paper is organized as follows: Section II introduces the CVaR-based definition of reserve capacities caused by WPFE. The DRCRS model with wind power is presented in Section III. Section IV gives the reformulation procedure of the CVaR-based wind power capacity and the distributionally robust chance constraint. Section V and VI provide the algorithm and case studies, respectively. Finally, conclusions are drawn in Section VII.

II. CVaR-Based Wind Power Reserve Capacity

To maintain the security of power system, the system operator has to prepare a certain level of extra reserve for the wind power uncertainty. In this section, the distributionally robust decision method of wind power reserve based on the concept of CVaR is introduced.

As a risk measure in finance, CVaR at $q\%$ level is defined to be the expected loss of the portfolio in the worst $q\%$ cases [24]. It is an alternative to VaR, which is defined as a threshold loss value, such that the probability that the loss exceeds this value is $q\%$ [25].

If the specific distribution of wind power forecast error is known, then similar to the concept of CVaR, the wind power reserve capacity at α risk level can be defined as the expected reserve requirement in the worst α cases [4], [5], that is,

$$R_{C_\alpha,t} = \alpha^{-1} \int_{R(\boldsymbol{\xi}) \geq \delta} R(\boldsymbol{\xi})\, \phi(\boldsymbol{\xi})\, d\boldsymbol{\xi} \tag{1}$$

where the random variable WPFE denoted as $\boldsymbol{\xi}$ is a continuous random variable; $R(\boldsymbol{\xi}) = \max(0, -\mathbf{1}^T\boldsymbol{\xi})$ denotes the up reserve, and $R(\boldsymbol{\xi}) = \max(0, \mathbf{1}^T\boldsymbol{\xi})$ denotes the down reserve. Similarly, δ is defined as the concept of VaR, a threshold amount of reserve so that the probability of wind power reserve requirement exceeding this amount is $\alpha\,(0 < \alpha \leq 1)$, it can be calculated as

$$\delta = \underset{\delta \in R^1}{inf} \left\{ \int_{R(\boldsymbol{\xi}) \geq \delta} \phi(\boldsymbol{\xi})\, d\boldsymbol{\xi} \leq \alpha \right\} \tag{2}$$

Since $R_{C_\alpha,t}$ takes into account the probability distribution of the reserve requirement that exceeds δ, it is more conservative and reliable compared to δ.

Further, consider that the exact PD of WPFE in different wind farms is unknown, and only the mean vector $\boldsymbol{\mu}$ and covariance matrix $\boldsymbol{\Gamma}$ of WPFE are available, then the CVaR-based wind power reserve capacity at α level needs to be redefined as

$$R_{C_\alpha,t} = \sup_{\phi \in \Phi(\mu,\Gamma)} \alpha^{-1} \int_{R(\boldsymbol{\xi}) \geq \delta} R(\boldsymbol{\xi})\, \phi(\boldsymbol{\xi})\, d\boldsymbol{\xi} \tag{3}$$

where the set $\Phi(\boldsymbol{\mu}, \boldsymbol{\Gamma})$ contains all the PDs that are consistent with the information of $\boldsymbol{\mu}$ and $\boldsymbol{\Gamma}$, it is defined as

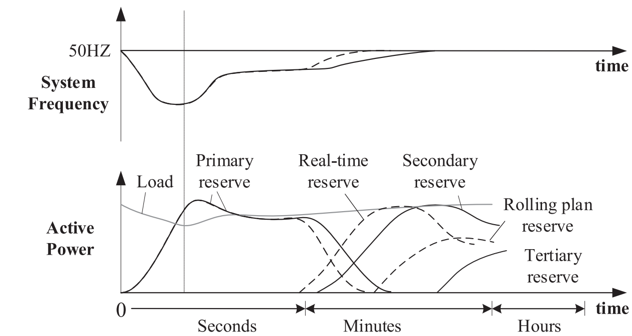

Fig. 1. Coordination of various reserves.

$$\Phi(\boldsymbol{\mu}, \boldsymbol{\Gamma}) = \left\{ \phi(\boldsymbol{\xi}) \left| \begin{array}{l} \int \phi(\boldsymbol{\xi})\, d\boldsymbol{\xi} = 1, \phi(\boldsymbol{\xi}) \geq 0 \\ \int \boldsymbol{\xi}\phi(\boldsymbol{\xi})\, d\boldsymbol{\xi} = \boldsymbol{\mu} \\ \int \boldsymbol{\xi}\boldsymbol{\xi}^T \phi(\boldsymbol{\xi})\, d\boldsymbol{\xi} = \boldsymbol{\Gamma} \end{array} \right. \right\}$$

The CVaR-based wind power reserve can lay a foundation for the distributionally robust decision method proposed below. The idea behind the definition (3) is that the probability of the real-time wind power reserve requirement exceeding the CVaR reserve capacity (if retained by system operator) will not be larger than α, over all possible PDs of WPFE. With the introduction of the PD uncertainty of WPFE, and a balance between reliability and economy of the decision on wind power reserve capacities can thus be realized.

III. Distributionally Robust Coordinated Reserve Scheduling Model With Wind Power

Conventionally, the operating reserve of power system is used to smooth the fluctuation of power load and meet the demand in case that any system component fails. According to its activation time, the operating reserve can be typically classified into three categories: primary reserve, secondary reserve and tertiary reserve [26]. The primary reserve is the generation capacity that is activated automatically within 30 seconds by the fluctuation of system frequency. The secondary reserve refers to the power capacity activated in $10{\sim}15$ minutes, which will be activated almost after the primary reserve and last until the tertiary reserve alternate with it. The tertiary reserve is activated lastly in hour time scale. An illustration of these three reserves is given in Fig. 1.

With the increasing penetration of wind power, more rapidly responded and frequently coordinated reserves are desired to smooth the volatility of wind power [4], [7]. And there is great concern on more fine-grained reserve scheduling to cover the rolling-plan reserve with 15-minute execution cycle and even the real-time reserve with 5-minute execution cycle [27], as illustrated in the dash curves of Fig. 1 [4]. The real-time reserve can play an important role of reducing the power mismatch caused by the load fluctuation and WPFE. The real-time reserve is mostly provided by fast response generators, e.g., gas turbine units and hydro storage plants. The rolling-plan reserve is used to replace any possible failed system component and provide continuous support after the real-time reserve. It should be noted that those generators that act as the real-time reserve roles can also provide the rolling-plan reserves as needed, since the latter is activated later than the former.

In this paper, the reserve framework composed of three types of reserves introduced above will be utilized for the purpose of wind power accommodation: the primary reserve, the real-time reserve and the rolling-plan reserve. The objective of reserve scheduling is to minimize the cost of power generation and reserve procurement with uncertain wind power, while maintaining the security of the power system. Since the primary reserve is automatically finished in seconds, it is not included in the reserve scheduling. For each time period $t = 1, \ldots, N_t$, the decision variables are grouped as compact vector form:

$$\begin{aligned}\mathbf{x_t} = [&P_{G1,t}, \ldots, P_{GN_G,t}, \lambda_{G1,t}^{up,rt}, \ldots, \lambda_{GN_{RT},t}^{up,rt}, \lambda_{G1,t}^{dn,rt}, \ldots,\\ &\lambda_{GN_{RT},t}^{dn,rt}, d_{G1,t}^{rt}, \ldots, d_{GN_{RT},t}^{rt}, \lambda_{G1,t}^{up,rp}, \ldots, \lambda_{GN_{RP},t}^{up,rp},\\ &\lambda_{G1,t}^{dn,rp}, \ldots, \lambda_{GN_{RP},t}^{dn,rp}]^T \end{aligned} \tag{4}$$

where $d_{Gj,t}^{rt}$, $j \in \Omega_{RT}$ indicates the allocation strategy of the real-time reserve.

Consider the uncertainty on the PD of WPFE, as well as the conventional generation ramping limits, the single-period DRCRS model is formulated as follows.

$$\begin{aligned}\min_{x_t} f_t(\boldsymbol{x_t}) &= \sum_{i\in\Omega_G} (a_{1i} P_{Gi,t})\\ &+ \sum_{j\in\Omega_{RT}} \left(a_{Gj}^{up,rt} \lambda_{Gj,t}^{up,rt} \bar{r}_{Gj}^{up} T_5 + a_{Gj}^{dn,rt} \lambda_{Gj,t}^{dn,rt} \bar{r}_{Gj}^{dn} T_5 \right)\\ &+ \sum_{k\in\Omega_{RP}} \left(a_{Gk}^{up,rp} \lambda_{Gk,t}^{up,rp} \bar{r}_{Gk}^{up} T_{15} + a_{Gk}^{dn,rp} \lambda_{Gk,t}^{dn,rp} \bar{r}_{Gk}^{dn} T_{15} \right)\end{aligned} \tag{5}$$

Subject to the following constraints.

1) *The forecasting power balance constraint:*

$$\sum_{i\in\Omega_G} P_{Gi,t} + \sum_{i\in\Omega_W} P_{Wi,t}^f = \sum_{i\in\Omega_D} P_{Di,t} \tag{6}$$

which indicates that the power balance in the system should be satisfied when the actual wind power $P_{Wk,t}$ equals to the forecasted value $P_{Wi,t}^f, i \in \Omega_W$.

2) *The generation limits:* $\forall i \in \Omega_G$

$$\underline{P}_{Gi} \le P_{Gi,t} \le \bar{P}_{Gi} \tag{7}$$

3) *The generation ramping limits:* $\forall i \in \Omega_G$

$$-\bar{r}_{Gi}^{dn} \Delta T \le P_{G,t} - P_{Gi,t-1} \le \bar{r}_{Gi}^{up} \Delta T \tag{8}$$

4) *The forecasting active line flow limits:* $\forall l \in \Omega_L$

$$\underline{P}_{Ll} \le P_{Ll,t}^f \le \bar{P}_{Ll} \tag{9}$$

with $\begin{cases} \boldsymbol{P_{L,t}^f} = \boldsymbol{T P_t^f},\\ \boldsymbol{P_t^f} = \boldsymbol{C_G P_{G,t}} + \boldsymbol{C_W P_{W,t}^f} - \boldsymbol{C_D P_{D,t}} \end{cases}$

5) *The real-time reserve capacity limits:* $\forall j \in \Omega_{RT}$

$$\begin{cases} P_{Gj,t} + \lambda_{Gj,t}^{up,rt} \bar{r}_{Gj}^{up} T_5 \le \bar{P}_{Gj}\\ P_{Gj,t} - \lambda_{Gj,t}^{dn,rt} \bar{r}_{Gj}^{dn} T_5 \ge \underline{P}_{Gj} \end{cases} \tag{10}$$

$$\begin{cases} \sum_{j\in\Omega_{RT}} \lambda_{Gj,t}^{up,rt} \bar{r}_{Gj}^{up} T_5 \ge R_{\min}^{up,rt} = R_L^{up} + R_W^{up} & (11)\\ \sum_{j\in\Omega_{RT}} \lambda_{Gj,t}^{dn,rt} \bar{r}_{Gj}^{dn} T_5 \ge R_{\min}^{dn,rt} = R_L^{dn} + R_W^{dn} & (12) \end{cases}$$

$$\begin{cases} 0 \le \lambda_{Gj,t}^{up,rt} \le 1,\\ 0 \le \lambda_{Gj,t}^{dn,rt} \le 1 \end{cases} \tag{13}$$

where $\lambda_{Gj,t}^{up,rt} \bar{r}_{Gj}^{up} T_5$ and $\lambda_{Gj,t}^{dn,rt} \bar{r}_{Gj}^{dn} T_5$ are the up and down reserve capacities procured from the jth real-time reserve unit. R_W^{up} and R_W^{dn} are the required up and down reserve capacity for WPFE, determined by the distributionally robust CVaR-based method in Section II.

6) *The rolling-plan reserve capacity limits:* $\forall k \in \Omega_{RP}$

$$\begin{cases} P_{Gk,t} + \lambda_{Gk,t}^{up,rp} \bar{r}_{Gk}^{up} T_{15} \le \bar{P}_{Gk},\\ P_{Gk,t} - \lambda_{Gk,t}^{dn,rp} \bar{r}_{Gk}^{dn} T_{15} \ge \underline{P}_{Gk} \end{cases} \tag{14}$$

$$\begin{cases} \sum_{k\in\Omega_{RP}} \lambda_{Gk,t}^{up,rp} \bar{r}_{Gk}^{up} T_{15} \ge R_{\min}^{up,rp} = R_{sys}^{up} + R_{\min}^{up,rt},\\ \sum_{k\in\Omega_{RP}} \lambda_{Gk,t}^{dn,rp} \bar{r}_{Gk}^{dn} T_{15} \ge R_{\min}^{dn,rp} = R_{sys}^{dn} + R_{\min}^{dn,rt} \end{cases} \tag{15}$$

$$\begin{cases} 0 \le \lambda_{Gk,t}^{up,rp} \le 1,\\ 0 \le \lambda_{Gk,t}^{dn,rp} \le 1 \end{cases} \tag{16}$$

7) *The real-time power system security constraints:*

$$\begin{aligned}\inf_{\phi\in\Phi(\mu,\Gamma)} \Pr &\left\{ \begin{array}{l} \underline{P}_{Ll} \le P_{Ll,t}^{rt} \le \bar{P}_{Ll},\\ -\lambda_{Gj,t}^{dn,rt} \bar{r}_{Gj}^{dn} T_5 \le R_{Gj,t}^{rt} \le \lambda_{Gj,t}^{up,rt} \bar{r}_{Gj}^{up} T_5,\\ \quad \forall l \in \Omega_L, \forall j \in \Omega_{RT} \end{array} \right\}\\ &\ge 1 - \beta \end{aligned} \tag{17}$$

with

$$\begin{cases} \boldsymbol{P_{L,t}^{rt}} = \boldsymbol{T P_t^{rt}},\\ \boldsymbol{P_t^{rt}} = \boldsymbol{C_G P_{G,t}} + \boldsymbol{C_{RT} R_{G,t}^{rt}} + \boldsymbol{C_W P_{W,t}}\\ \qquad - \boldsymbol{C_D P_{D,t}},\\ \boldsymbol{R_{G,t}^{rt}} = \boldsymbol{d_{G,t}^{rt}} \cdot \boldsymbol{1^T \xi},\\ \boldsymbol{1^T} \cdot \boldsymbol{d_{G,t}^{rt}} = -1 \text{ or } \sum_{j\in\Omega_{RT}} d_{Gj,t}^{rt} = -1 \end{cases} \tag{18}$$

The first constraint in (17) indicates the active power flow limits on each transmission line. The second constraint in (17) indicates that the reserve is limited by the procured capacity.

In the DRCRS model, the decision variables $P_{Gi,t}$, $i \in \Omega_G$ is the optimal generation dispatch. The real-time reserve procurement factors $\lambda_{Gj,t}^{up,rt}$ and $\lambda_{Gj,t}^{dn,rt}$, $j \in \Omega_{RT}$ can determine the up and down reserve capacities procured from each participant generator. Similarly, the rolling-plan reserve procurement factors $\lambda_{Gk,t}^{up,rp}$ and $\lambda_{Gk,t}^{dn,rp}$, $k \in \Omega_{RP}$ can determine the rolling-plan reserve capacities procured. Here $\mathbf{1}^T \cdot \boldsymbol{d_{G,t}^{rt}} = -1$ with $-1 \le d_{Gj,t}^{rt} \le 0$ indicates that the total reserve arranged are used to inversely compensate the varaiation of $\boldsymbol{\xi}$, in which the allocation percentage of the total real-time reserve among all participant generators.

In particular, constraint (17) takes into account the uncertainty on the PD of WPFE, and its physical meaning is that under any possible PD of WPFE, the probability of transmission line overload or WPFE reserve insufficiency will not exceed the predefined risk level. Therefore, this constraint is indeed a distributionally robust joint chance constraint [23], [28], which is, however, difficult to be handled in real applications. Moreover, in constraints (11) and (12), the total reserve requirements caused by WPFE, R_W^{up} and R_W^{dn}, need to be determined in advance according to the CVaR concept in (3), with $R(\boldsymbol{\xi}) = \max(0, -\mathbf{1}^T\boldsymbol{\xi})$ for the up reserve and $R(\boldsymbol{\xi}) = \max(0, \mathbf{1}^T\boldsymbol{\xi})$ for the down reserve.

IV. Tractable Problem Reformulations

To achieve tractability of the DRCRS model, the reserve requirements for WPFE, R_W^{up} and R_W^{dn}, will be converted into a LMI problem in subsection A; In subsection B, the S-lemma [21] and the Schur complements [23] will be used to convert the probabilistic constraint (17) into BMIs.

A. Calculation of CVaR-Based Wind Power Reserve Capacities

Take R_W^{up} for an example, based on the formulation of CVaR [24], it can be rewritten as

$$\begin{aligned} R_W^{up} &= \sup_{\phi\in\Phi(\mu,\Gamma)} \alpha^{-1}\int_{(-\mathbf{1}^T\boldsymbol{\xi})^+\geq\delta} (-\mathbf{1}^T\boldsymbol{\xi})^+\phi(\boldsymbol{\xi})\,d\boldsymbol{\xi} \\ &= \sup_{\phi\in\Phi(\mu,\Gamma)} \inf_{\delta\in R^1}\left\{\delta+\alpha^{-1}E\left[\left((-\mathbf{1}^T\boldsymbol{\xi})^+-\delta\right)^+\right]\right\} \\ &= \inf_{\delta\in R^1}\left\{\delta+\alpha^{-1}\sup_{\phi\in\Phi(\mu,\Gamma)} E\left[\left((-\mathbf{1}^T\boldsymbol{\xi})^+-\delta\right)^+\right]\right\} \end{aligned} \tag{19}$$

where $(-\mathbf{1}^T\boldsymbol{\xi})^+ = \max\left(0, -\mathbf{1}^T\boldsymbol{\xi}\right)$, $E[x]$ denotes the expected value of x.

From the duality theory [28], $\sup_{\phi\in\Phi(\mu,\Gamma)} E[((-1^T\boldsymbol{\xi})^+-\delta)^+]$ in (19) corresponds to the objective value in (20), with the proof process given in Appendix A.

$$\begin{aligned} &\inf_{\boldsymbol{M_R}={\boldsymbol{M_R}}^T\in R^{(n+1)\times(n+1)}} Trace\,(\boldsymbol{QM_R}) \\ &s.t.\ \left[\,\boldsymbol{\xi}^T\ 1\,\right]\boldsymbol{M_R}\left[\,\boldsymbol{\xi}^T\ 1\,\right]^T \geq \left(\left(-\mathbf{1}^T\boldsymbol{\xi}\right)^+-\delta\right)^+, \forall\boldsymbol{\xi}\in R^n \end{aligned} \tag{20}$$

where $\boldsymbol{M_R}$ is defined as a symmetric matrix consists of the dual variables, and

$$\boldsymbol{Q} = \begin{bmatrix} \boldsymbol{\Gamma}+\boldsymbol{\mu}\boldsymbol{\mu}^T & \boldsymbol{\mu} \\ \boldsymbol{\mu}^T & 1 \end{bmatrix}.$$

In addition, the constraint in (20) can be expanded into the following constraints.

$$\begin{cases} \left[\,\boldsymbol{\xi}^T\ 1\,\right]\boldsymbol{M_R}\left[\,\boldsymbol{\xi}^T\ 1\,\right]^T \geq 0, & \forall\boldsymbol{\xi}\in R^n \\ \left[\,\boldsymbol{\xi}^T\ 1\,\right]\left(\boldsymbol{M_R}+\begin{bmatrix}\mathbf{0}_{n\times n} & \mathbf{0}_n \\ \mathbf{0}_n^T & \delta\end{bmatrix}\right)\begin{bmatrix}\boldsymbol{\xi}\\1\end{bmatrix} \geq 0, & \forall\boldsymbol{\xi}\in R^n \\ \left[\,\boldsymbol{\xi}^T\ 1\,\right]\left(\boldsymbol{M_R}+\begin{bmatrix}\mathbf{0}_{n\times n} & (\mathbf{1/2})_n \\ (\mathbf{1/2})_n^T & \delta\end{bmatrix}\right)\begin{bmatrix}\boldsymbol{\xi}\\1\end{bmatrix} \geq 0, & \forall\boldsymbol{\xi}\in R^n \end{cases} \tag{21}$$

where $\mathbf{0}_{n\times n}$ denotes an $n\times n$-dimension zero matrix, and $(\mathbf{1/2})_n$ denotes an n-dimension vector in which each element is 1/2. Thus, the random vector $\boldsymbol{\xi}$ can be eliminated directly, and (21) is converted into

$$\begin{cases} \boldsymbol{M}_R \geq 0, \\ \boldsymbol{M_R} + diag\left(\left[\mathbf{0}_n^T,\delta\right]\right) \geq 0, \\ \boldsymbol{M_R} + \begin{bmatrix}\mathbf{0}_{n\times n} & (\mathbf{1/2})_n \\ (\mathbf{1/2})_n^T & \delta\end{bmatrix} \geq 0 \end{cases} \tag{22}$$

where diag(x) denotes a diagonal matrix in which the diagonal elements compose the vector x.

From the above derivation, R_W^{up} corresponds to the objective value of the following LMI problem:

$$\begin{aligned} R_W^{up} &= \inf_{\delta\in R^1}\delta+\alpha^{-1}Trace\,(\boldsymbol{QM_R}) \\ &s.t.\ \boldsymbol{M}_R = {\boldsymbol{M}_R}^T \in R^{(n+1)\times(n+1)}, \\ &\begin{cases} \boldsymbol{M_R} \geq 0, \\ \boldsymbol{M}_R + diag\left(\left[\mathbf{0}_n^T,\delta\right]\right) \geq 0, \\ \boldsymbol{M_R} + \begin{bmatrix}\mathbf{0}_{n\times n} & (\mathbf{1/2})_n \\ (\mathbf{1/2})_n^T & \delta\end{bmatrix} \geq 0 \end{cases} \end{aligned} \tag{23}$$

Similarly, R_W^{dn} can be expressed as the objective value of a tractable LMI problem as well.

B. Reformulation of the Distributionally Robust Joint Chance Constraint

The S-lemma is applied to eliminate the random vector $\boldsymbol{\xi}$ in (17), which is an implicit variable in the active line power flow $P_{Ll,t}^{up}$ and $P_{Ll,t}^{dn}$; moreover, by using the Schur complements, constraint (17) can be further transformed into BMIs. The procedures are described as follows.

Rewrite each individual constraint inside the probability of (17) in a quadratic form. For example, according to (18), $R_{Gj,t}^{rt} - \lambda_{Gj,t}^{up,rt}\bar{r}_{Gj}^{up}T_5$ can be calculated as

$$R_{Gj,t}^{rt} - \lambda_{Gj,t}^{up,rt}\bar{r}_{Gj}^{up}T_5 = {\boldsymbol{L_{upj}}}^T(\boldsymbol{x}_t)\,\boldsymbol{\xi} + L_{upj}^0(\boldsymbol{x_t}) \tag{24}$$

where $\boldsymbol{L_{upj}}(\boldsymbol{x_t})$ is an n-dimension column vector in which each element is a linear function of the decision variable $\boldsymbol{x_t}$ in (4), and the scalar $L_{upj}^0(\boldsymbol{x_t})$ is also a linear function of $\boldsymbol{x_t}$.

Secondly, by introducing a large enough constant ρ, the individual constraint of $R_{Gj,t}^{rt} - \lambda_{Gj,t}^{up,rt}\bar{r}_{Gj}^{up}T_5 \leq 0$ is expressed as,

$$\begin{aligned} &-2\rho \leq {\boldsymbol{L_{upj}}}^T(\boldsymbol{x}_t)\,\boldsymbol{\xi} + L_{upj}^0(\boldsymbol{x_t}) \leq 0 \\ &\Leftrightarrow \left(\left[\,{\boldsymbol{L_{upj}}}^T(\boldsymbol{x}_t)\ \ L_{upj}^0(\boldsymbol{x_t})+\rho\,\right]\begin{bmatrix}\boldsymbol{\xi}\\1\end{bmatrix}\right)^2 \leq \rho^2 \end{aligned} \tag{25}$$

where $\Leftrightarrow$ denotes the equivalent conversion. Therefore, (17) can be written into the following general form:

$$P_{WC}\left(\boldsymbol{x}_t\right) = \sup_{\phi\in\Phi(\mu,\Gamma)} \Pr\left(\bigcup_{k=1}^{N_L+2N_{RT}} \left\{\left[\boldsymbol{F}_k\left(\boldsymbol{x}_t\right)\boldsymbol{z}\right]^2 \geq \gamma_k^2\right\}\right) \leq \beta \tag{26}$$

where $\boldsymbol{F_k}\left(\boldsymbol{x_t}\right), k=1,\ldots,N_L+N_{RT}$ is an $(n+1)$-dimension row vector in which each element is a linear function of $\boldsymbol{x_t}$; $\boldsymbol{z}=\begin{bmatrix}\boldsymbol{\xi}^T & 1\end{bmatrix}^T$, and $\gamma_k, k=1,\ldots,N_L+N_{RT}$ is a constant.

According to the duality theory [29], $P_{WC}\left(\boldsymbol{x_t}\right)$ in the left side of (26) equals to the objective value of subproblem (27)–(29), with the proof process given in Appendix B.

$$P_{WC}\left(\boldsymbol{x_t}\right) = \underset{M=M^T\in R^{(n+1)\times(n+1)}}{inf} Trace\left(\boldsymbol{QM}\right) \tag{27}$$

$$s.t. \quad \boldsymbol{M} \geq 0, \tag{28}$$

$$\boldsymbol{z}^T\boldsymbol{Mz} \geq 1, \forall \boldsymbol{z} : \left[F_k\left(\boldsymbol{x}_t\right)\boldsymbol{z}\right]^2 \geq \gamma_k^2,\ k=1,\ldots,N_L+2N_{RT} \tag{29}$$

where $\boldsymbol{M}$ is defined to be a symmetric matrix consisting of the dual variables.

By the S-lemma [21], (29) can be strictly converted into the following deterministic constraint:

$$\begin{cases} \exists\tau_k \geq 0, \\ \boldsymbol{M} - diag\left(\boldsymbol{0}_n, 1-\tau_k\gamma_k^2\right) - \tau_k {\boldsymbol{F}_k}^T\left(\boldsymbol{x}_t\right)\boldsymbol{F}_k\left(\boldsymbol{x}_t\right) \geq 0 \end{cases} \tag{30}$$

Further, by the Schur complements [22], (30) can be transformed into the form of (31),

$$\begin{cases} \exists\tau_k \geq 0, \\ \begin{bmatrix} \boldsymbol{M} - diag\left(\boldsymbol{0}_n, 1-\tau_k\gamma_k^2\right) & \tau_k {\boldsymbol{F}_k}^T\left(\boldsymbol{x}_t\right) \\ \tau_k\boldsymbol{F}_k\left(\boldsymbol{x}_t\right) & \tau_k \end{bmatrix} \geq 0 \end{cases} \tag{31}$$

Thus, subproblem (27)–(29) is equivalently converted into the following optimization problem:

$$P_{WC}\left(\boldsymbol{x}_t\right) = \inf_{M=M^T\in R^{(n+1)\times(n+1)},\tau_k} Trace\left(\boldsymbol{QM}\right) \tag{32}$$

$$s.t. \quad \boldsymbol{M} \geq 0, \tag{33}$$

$$\tau_k \geq 0, \tag{34}$$

$$\begin{bmatrix} \boldsymbol{M} - diag\left(\boldsymbol{0}_n, \boldsymbol{1}-\tau_k\gamma_k^2\right) & \tau_k\boldsymbol{F}_k^T(\boldsymbol{x}_t) \\ \tau_k\boldsymbol{F}_k(\boldsymbol{x}_t) & \tau_k \end{bmatrix} \geq 0 \tag{35}$$

$$k=1,\ldots,N_L+2N_{RT} \tag{36}$$

Meanwhile, the probabilistic constraint (17) is converted into the deterministic BMI form of (37), which contains the bilinear term $\tau_k\boldsymbol{F_k}\left(\boldsymbol{x_t}\right)$.

$$\begin{cases} Trace\left(\boldsymbol{QM}\right) \leq \beta \\ \boldsymbol{M} = \boldsymbol{M}^T \in R^{(n+1)\times(n+1)}, \\ M \geq 0, \\ \tau_k \geq 0, \\ \begin{bmatrix} \boldsymbol{M} - diag\left(\boldsymbol{0}_n, 1-\tau_k\gamma_k^2\right) & \tau_k {\boldsymbol{F}_k}^T\left(\boldsymbol{x}_t\right) \\ \tau_k\boldsymbol{F}_k\left(\boldsymbol{x}_t\right) & \tau_k \end{bmatrix} \geq 0 \\ k=1,\ldots,N_L+2N_{RT} \end{cases} \tag{37}$$

C. Deterministic Model of the DRCRS Problem

From the above derivation, it can be found that the random vector $\boldsymbol{\xi}$ in the DRCRS model (5)–(18) can be strictly eliminated, and the resulting deterministic model is a BMI-constrained optimization problem as follows, in which the 15-minute ramping limits (39) are used to replace (8).

$$\begin{aligned} \min_{x_t} f_t(x_t) = &\sum_{i\in\Omega_G}\left(a_{1i}P_{Gi,t}\right) \\ &+ \sum_{j\in\Omega_{RT}}\left(a_{Gj}^{up,rt}\lambda_{Gj,t}^{up,rt}\bar{r}_{Gj}^{up}T_5 + a_{Gj}^{dn,rt}\lambda_{Gj,t}^{dn,rt}\bar{r}_{Gj}^{dn}T_5\right) \\ &+ \sum_{k\in\Omega_{RP}}\left(a_{Gk}^{up,rp}\lambda_{Gk,t}^{up,rp}\bar{r}_{Gk}^{up}T_{15} + a_{Gk}^{dn,rp}\lambda_{Gk,t}^{dn,rp}\bar{r}_{Gk}^{dn}T_{15}\right) \end{aligned} \tag{38}$$

s.t. (6)–(7), (9)–(16)

$$-\bar{r}_{Gk}^{dn}T_{15} \leq P_{Gk,t} - P_{Gk,t-1} \leq \bar{r}_{Gk}^{up}T_{15}, k\in\Omega_{RP} \tag{39}$$

$$\begin{cases} Trace\left(\boldsymbol{Q}\cdot\boldsymbol{M}\right) \leq \beta \\ \boldsymbol{M} = \boldsymbol{M}^T \in \boldsymbol{R}^{(n+1)\times(n+1)}, \\ \boldsymbol{M} \geq 0, \\ \tau_k \geq 0, \\ \begin{bmatrix} \boldsymbol{M} - diag\left(\boldsymbol{0}_n, 1-\tau_k\gamma_k^2\right) & \tau_k {\boldsymbol{F}_k}^T\left(\boldsymbol{x}_t\right) \\ \tau_k\boldsymbol{F}_k\left(\boldsymbol{x}_t\right) & \tau_k \end{bmatrix} \geq 0 \\ k=1,\ldots,N_L+2N_{RT} \end{cases} \tag{40}$$

The BMI problems are nonconvex and difficult to be solved. In the next section, the sequential convex optimization algorithm [23], [28] will be introduced to achieve the tractability of the BMI problem (38)–(40).

V. Algorithm of BMI-Problem

The single-period optimization model (38)–(40) will be independently solved for each time period, and the generation and reserve scheme obtained by the last time period model will be used as an initial condition for the next time period.

The key to solving the BMI-P is to deal with the bilinear terms $\tau_k\boldsymbol{F_k}\left(\boldsymbol{x_t}\right),\ k=1,\ldots,N_L+2N_{RT}$ in (40). The main idea of the sequential convex optimization algorithm [23], [28] is to optimize $\boldsymbol{\tau}=\{\tau_k, k=1,\ldots,N_L+2N_{RT}\}$ and $\boldsymbol{x_t}$ in alternation, which is realized by solving a sequence of LMI constrained problems. The specific procedures are as follows:

1) **Initialization:** Set the initial solution to some feasible value $\boldsymbol{x_t^1}$, the corresponding objective value is denoted as f^1, and let the iteration counter m $= 1$.
2) **Parameter optimization:** Substitute $\boldsymbol{x_t}=\boldsymbol{x_t^m}$ into subproblem (32)–(36). Solve the resulting LMI problem and obtain the optimal solution $\boldsymbol{\tau}^*$. Set $\boldsymbol{\tau}^m=\boldsymbol{\tau}^*$.
3) **Optimal decision:** Substitute $\boldsymbol{\tau}=\boldsymbol{\tau}^m$ into the BMI problem (38)–(40). Solve the resulting LMI problem and obtain the updated optimal solution $\boldsymbol{x_t^*}$ and the corresponding objective value f^*. Set $\boldsymbol{x_t^{m+1}}=\boldsymbol{x_t^*}$, $f^{m+1}=f^*$.

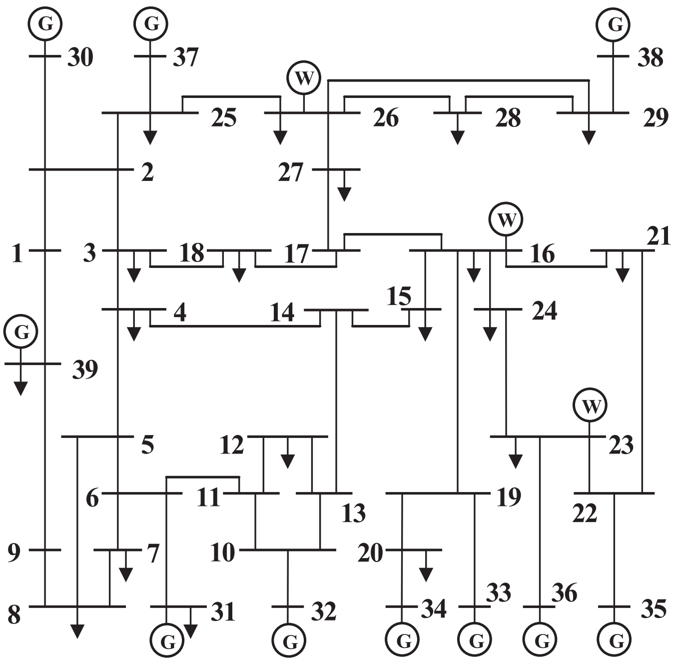

Fig. 2. Diagram of the IEEE 39-bus system with three wind farms.

4) **Termination:** If $\left|f^{m+1}-f^{m}\right|/\left|f^{m}\right| \le \varepsilon$, where ε is a predefined small tolerance, then the final optimums $\boldsymbol{x_t^{m+1}}$ and f^{m+1} are obtained, and the algorithm ends. Otherwise, let m $=$ m $+$ 1, and repeat Step 2)-4).

In the initialization step, a feasible solution can be obtained via the Bonferroni approximation in [28], the main idea is as follows: 1) Decompose the joint chance constraint of (17) into $N_L + 2N_{RT}$ individual chance constraints with risk levels $\beta_k = \beta/\left(N_L + 2N_{RT}\right)$ for $k = 1, \ldots, N_L + 2N_{RT}$; 2) convert individual chance constraint into a form similar to (37) but with only one BMI, which can be further converted into an LMI in this case [29]; 3) replace (17) with the resulting LMI constraints; finally, solve the LMI-constrained DRCRS model directly and obtain the initial solution for the sequential convex optimization algorithm.

Since $\boldsymbol{x_t}$ is bounded, in the sequential convex optimization algorithm, the sequence of objective values f^m is monotonically decreasing and converges to a finite limit. However, it should be noted that the sequential convex optimization algorithm is a heuristic algorithm and the final solution could be a local optimum due to the non-convexity of the BMI problems [28]. Despite of relative high computation effort, it is reported that some global optimization algorithm have potential to find the global optimum [30], whose performance can be further explored in the future work.

VI. Case Studies

The DRCRS method is tested on the IEEE 39-bus system illustrated in Fig. 2. Without loss of generality, three wind farms are assumed to be connected with the test system at bus 16, 23 and 26. It is assumed that all of the 10 conventional generators can provide the rolling-plan reserves, and only the generators at bus 30, 31, 35 and 38 have the ability to provide the real-time reserves. The conventional generators data are listed in Table I, and the minimum output is zero for each generator; the limits of up and down ramping rate are set to be equal, $\bar r_{Gi}^{up} = \bar r_{Gi}^{dn}$. All other system data including network data and load profiles can be referred in [31]. Both of the up and down reserve requirement, R_L^{up} and R_L^{dn}, are uniformly assumed to be 1% of the total system demand, i.e., 59.09 MW. The up reserve requirement for system contingency R_{sys}^{up} and the down reserve requirement R_{sys}^{dn} are both assumed to be 10% of the total system demand, i.e., 590.92 MW.

TABLE I
Parameters of the Conventional Generators

Unit	$\bar P_{Gi}$ (MW)	a_{1i} ($/MW)	r_{Gi}^{up} (MW/min)	$a_{Gj}^{up,rt}$ ($/MW)	$a_{Gj}^{dn,rt}$ ($/MW)	$a_{Gi}^{up,rp}$ ($/MW)	$a_{Gi}^{dn,rp}$ ($/MW)
G30	1040	0.3	50	0.35	0.50	0.35	0.50
G31	1050	0.3	50	0.45	0.40	0.45	0.40
G32	1050	0.3	30	-	-	0.30	0.25
G33	1050	0.3	40	-	-	0.28	0.22
G34	1050	0.3	30	-	-	0.32	0.30
G35	1050	0.3	50	0.40	0.45	0.40	0.45
G36	1260	0.3	20	-	-	0.30	0.28
G37	1050	0.3	30	-	-	0.25	0.22
G38	1060	0.3	50	0.50	0.35	0.50	0.35
G39	1060	0.3	20	-	-	0.28	0.30

An optimization time horizon of 6 hours is divided into 24 periods. The multiple-time data including the forecasted value,the mean and variance of the wind power output are listed in Appendix C. To simplify the analysis, the space correlation of different wind farms and the time correlation of wind power output at different time periods are ignored in the study.

In addition, when WPFE follows a normal distribution, then a special case of DRCRS method called the normal distribution based coordinated reserve scheduling (NDCRS), is also investigated here for comparison. The LMI problems embedded in the DRCRS model are solved by the SDPT3 solver via the YALMIP interface [32]. The NDCRS model is solved by the pattern search algorithm (PSA) [33] coded in MATLAB. Both of the two algorithm are performed in a computer platform with Intel Core I5 processor, with 2.80 GHz CPU and 8 GB RAM memory. It should be noted that PSA may trap in a local minimum and can be further improved by some global optimization methods, but PSA here can meet the goal of effect comparison between DRCRS and NDCRS.

A. Results Comparison Between DRCRS and NDCRS

The CVaR-based wind power reserves at each time period are presented in Fig. 3(a)–(b), with the confidence level $1-\alpha$ set to be 95%. It can be seen that both the up and the down wind power reserve considering distributionally robust (DR-WP case) are higher than the reserve requirements with WPFE of normal distribution (ND-WP case). The reason is that the former should respect all possible PDs of WPFE, instead of only

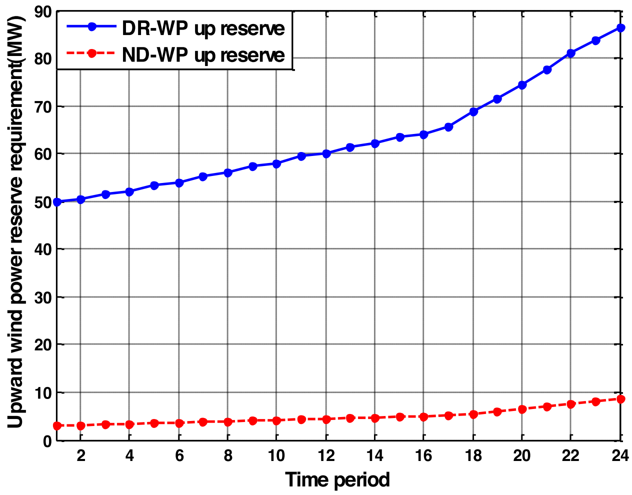

(a) the up reserve capacity

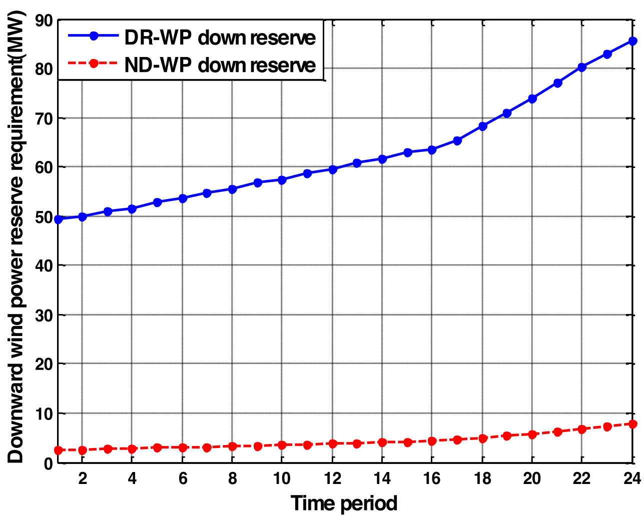

(b) the down reserve capacity

Fig. 3. The changes of wind power reserves in 24 time periods.

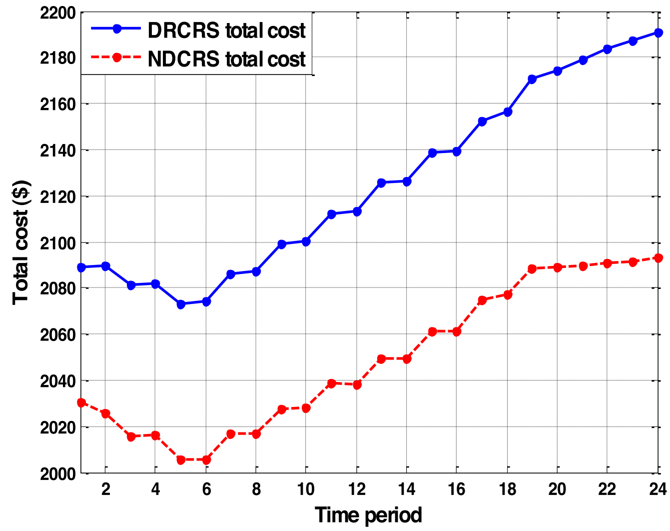

(a) the total reserve cost

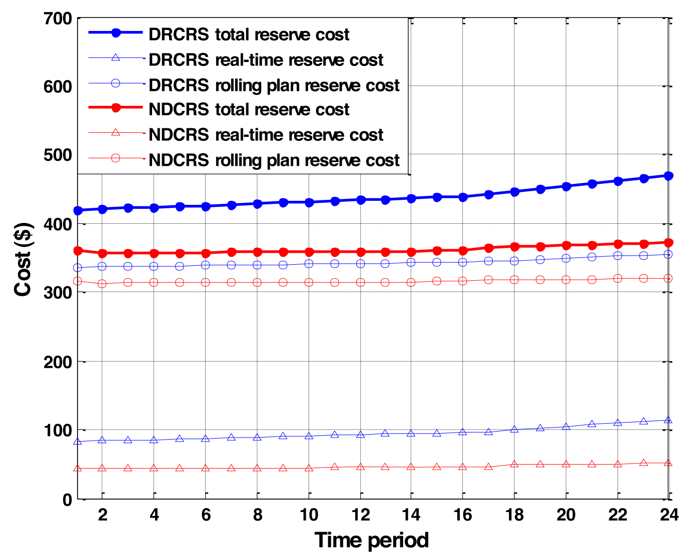

(b) the reserve cost details

Fig. 4. The resultant reserve costs comparison.

the normal distribution. In addition, both of two figures show that the requirement of wind power reserve increases over time. The main reason is that the variance of WPFE in each wind farm increases over time (as given in Appendix C), which indicates that when the uncertainty increases, the reserve requirements will increase accordingly.

Fig. 4(a) shows the total cost of conventional generation and reserve procurement at each time period, with the confidence level of the security constraint satisfaction $1-\beta$ set to be 95%. Fig. 4(b) shows the corresponding reserve procurement costs at each time period. The optimal solutions for the 1st time period are listed in Table II. It can be seen that the total cost obtained by the DRCRS method is higher than that obtained by the NDCRS model. The main reason is that the DRCRS model considers all possible PDs of WPFE, while the NDCRS model only takes the normal distribution of WPFE into account. From Fig. 4(a)–(b), it can also be seen that the difference between the total costs of DRCRS model and NDCRS model is mainly caused by the difference between the reserve costs of these two models.

B. Coordinated Reserve Scheduling With Different Confidence Levels and WPFE Variances

To evaluate the effect of the security constraint confidence level 1-β on the optimal results, the value of 1-β is increased from 90% to 99.94% at the time period $t=1$, and the total cost of conventional generation and reserve procurement are shown in Fig. 5. It can be seen that both of the total costs obtained by the DRCRS model and the NDCRS model increase. Especially, when 1-β reaches a high value (98.8%~99.94%), the total cost of DRCRS model increases significantly. The reason is that when the security requirement increases, more conventional generation and reserve are needed to prepare for the fluctuation of wind power.

Moreover, since the DRCRS model considers all the possible PDs of WPFE rather than only the normal distribution, the DRCRS cost increases faster than the NDCRS cost when 1-β increases (as shown in Fig. 5). This observation indicates that the uncertainty of PD affects the security and economy

TABLE II
COMPARISON OF THE OPTIMAL RESULTS OF DRCRS MODEL AND NDCRS MODEL AT THE 1ST TIME PERIOD

	DRCRS result						NDCRS result					
Unit	$P_{Gi,t}$ (MW)	$\lambda_{Gj,t}^{up,rt}$	$\lambda_{Gj,t}^{dn,rt}$	$\lambda_{Gi,t}^{up,rp}$	$\lambda_{Gi,t}^{dn,rp}$	$d_{Gj,t}^{rt}$	$P_{Gi,t}$ (MW)	$\lambda_{Gj,t}^{up,rt}$	$\lambda_{Gj,t}^{dn,rt}$	$\lambda_{Gi,t}^{up,rp}$	$\lambda_{Gi,t}^{dn,rp}$	$d_{Gj,t}^{rt}$
G30	692.68	0.4355	0.1975	0	0	-0.9971	670.81	0.2335	0.0009	0	0z	-0.3776
G31	645.85	0	0	0	0	0	519.37	0.0001	0.0797	0	0	-0.0466
G32	724.88	-	-	0	0	-	690.36	-	-	0.0023	0.0030	-
G33	651.64	-	-	0.0005	0.9848	-	622.63	-	-	0.0054	0.9997	-
G34	507.87	-	-	0	0	-	470.77	-	-	0.0246	0	-
G35	482.10	0.0006	0.0006	0	0	-0.0029	581.89	0.0148	0.0020	0	0	-0.5365
G36	208.25	-	-	0	0	-	263.12	-	-	0	0	-
G37	114.00	-	-	1.0000	0.2413	-	167.93	-	-	0.7596	0.1141	-
G38	686.71	0	0.2361	0	0	0	775.57	0.0001	0.1639	0	0	-0.0384
G39	850.24	-	-	0.8322	0	-	801.68	-	-	0.9867	0	-

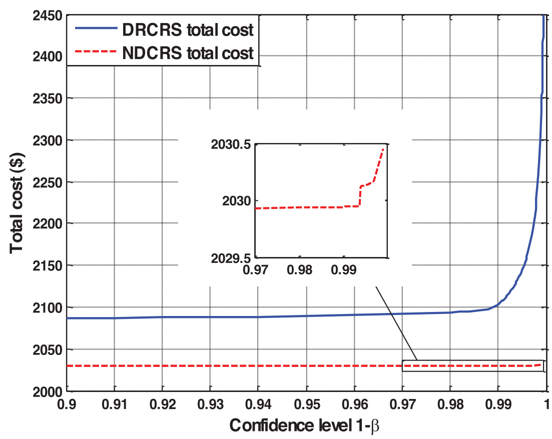

Fig. 5. Total cost with different confidence levels.

TABLE III
SOLUTION TIME FOR DRCRS MODEL AND NDCRS MODELE WITH DIFFERENT CONFIDENCE LEVELS

Confidence level		0.90	0.91	0.92	0.93	0.94	0.95
Solution time (s)	DRCRS	51	50	51	50	28	29
	NDCRS	482	413	478	506	482	495
Confidence level		0.96	0.97	0.98	0.99	0.995	0.998
Solution time (s)	DRCRS	28	29	29	33	36	45
	NDCRS	526	509	480	433	416	530

of the coordinated reserve scheduling significantly. In addition, Table III gives the solution time of the DRCRS model and the NDCRS model. It can be seen that both of these two models can be solved within 15 minutes and the DRCRS solution obviously has better computation efficiency.

To analyze the effect of the volatility of WPFE on the DRCRS optimal results, the standard deviation (root of the variance) of WPFE in each wind farm is multiplied by an adjust factor π ($\pi > 0$). The resulting total costs are shown in Fig. 6 where the value of π is increased from 0.4 to 1.6 with a step size of 0.2. It can be seen that with the increasing of variance, the total cost of generation and reserve procurement increases as well. This observation indicates that it costs more to keep the system security at a certain level when the volatility of WPFE increases.

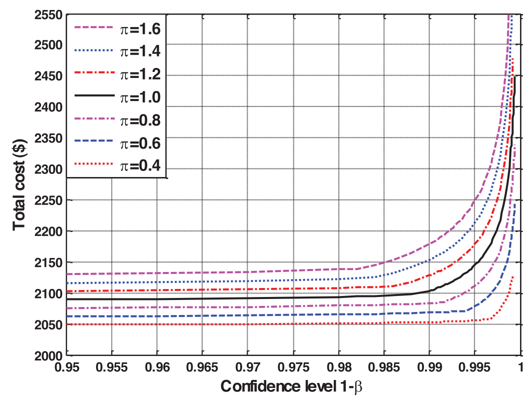

Fig. 6. Total cost with different variance.

VII. CONCLUSION

This paper proposed a DRCRS model to find a reserve scheduling solution that is robust to the uncertainty on the PD of WPFE, and minimize the total cost of conventional generation and reserve procurement. In this model, the capacity requirement of the wind power reserve are determined by a CVaR-based distributionally robust formulation, which means that the probability of the real-time wind power reserve exceeding the reserve capacity will not be larger than a certain level. Since the DRCRS model takes into account all possible PDs of WPFE, the total costs are always higher than those of the NDCRS model. In addition, the numerical results demonstrate that both of the system security confidence level and the WPFE volatility have some impacts on the total cost: 1) Higher system security requirement (reflected by the confidence level 1-β) leads to higher cost, and the cost increases significantly when some security level is reached; 2) higher wind power volatility (reflected by the WPFE variance) leads to higher cost.

The proposed distributionally robust optimization method could also be applied to solve other problems, such as reliability assessment and generation expansion. Future works could include the investigation of those global solution algorithms and the DRCRS model with more information given.

Appendixes

Appendix A

Proposition: $\sup\limits_{\phi\in\Phi(\mu,\Gamma)} E[((-\mathbf{1}^T\boldsymbol{\xi})^+-\delta)^+]$ corresponds to the objective value in the following equation,

$$\inf_{\boldsymbol{M_R}=\boldsymbol{M_R^T}\in R^{(n+1)\times(n+1)}} Trace\left(\boldsymbol{QM_R}\right)$$
$$s.t.\left[\,\boldsymbol{\xi}^T\ 1\,\right]\boldsymbol{M_R}\left[\,\boldsymbol{\xi}^T\ 1\,\right]^T \geq \left(\left(-1^T\boldsymbol{\xi}\right)^+-\delta\right)^+, \forall\boldsymbol{\xi}\in R^n$$

Proof [28]: The term $\mathop{sup}\limits_{\phi\in\Phi(\mu,\Gamma)} E[((-\mathbf{1}^T\boldsymbol{\xi})^+-\delta)^+]$ can be expressed as

$$\begin{cases} Z^P=\sup\limits_{\phi\in\mathcal{M}_+}\int\limits_{R^n}\left(\left(-1^T\boldsymbol{\xi}\right)^+-\delta\right)^+\phi\left(d\boldsymbol{\xi}\right) \\ \text{s.t.}\quad \int\limits_{R^n}\phi\left(d\boldsymbol{\xi}\right)=1 \\ \qquad \int\limits_{R^n}\boldsymbol{\xi}\phi\left(d\boldsymbol{\xi}\right)=\boldsymbol{\mu} \\ \qquad \int\limits_{R^n}\boldsymbol{\xi}\boldsymbol{\xi}^T\phi\left(d\boldsymbol{\xi}\right)=\boldsymbol{\Gamma}+\boldsymbol{\mu}\boldsymbol{\mu}^T \end{cases} \tag{A.1}$$

where $\mathcal{M}_+$ denotes the cone of nonnegative Borel measures on R^n, and the optimization variable of (A.1) is the measure ϕ. Due to the first constraint, ϕ must be a probability measure; the other two constraints force ϕ to fit the first and second moment information.

According to the duality theory, the following problem (A.2) is the dual problem of (A.1), at the same time, strong duality holds: $Z^P=Z^D$.

$$Z^D=\inf_{y_0,\mathbf{y},\mathbf{Y}} y_0+\boldsymbol{y}^T\boldsymbol{\mu}+Trace\left(\boldsymbol{\Gamma}+\boldsymbol{\mu}\boldsymbol{\mu}^T\right)\boldsymbol{Y} \tag{A.2}$$

s.t., $y_0+\boldsymbol{y}^T\boldsymbol{\xi}+Trace(\boldsymbol{\xi}\boldsymbol{\xi}^TY)\geq\left(\left(-\mathbf{1}^T\boldsymbol{\xi}\right)^+-\delta\right)^+, \forall\boldsymbol{\xi}\in R^n$ where $y_0\in R^1, \boldsymbol{y}\in R^n, \boldsymbol{Y}=\boldsymbol{Y}^T\in R^{n\times n}$ are the dual variables assigned to the first, the second and the third constraints in (A.1), respectively.

Further, we define $\mathbf{M}_R=\begin{bmatrix}\boldsymbol{Y} & \frac{1}{2}\boldsymbol{y}\\ \frac{1}{2}\boldsymbol{y}^T & y_0\end{bmatrix}$, $\mathbf{Q}=\begin{bmatrix}\boldsymbol{\Gamma}+\boldsymbol{\mu}\boldsymbol{\mu}^T & \boldsymbol{\mu}\\ \boldsymbol{\mu}^T & 1\end{bmatrix}$,
Then (A.2) can be written as

$$\inf_{\boldsymbol{M_R}=\boldsymbol{M_R^T}\in R^{(n+1)\times(n+1)}} Trace\left(\boldsymbol{QM_R}\right)$$
$$s.t.\quad \left[\,\boldsymbol{\xi}^T\ 1\,\right]\boldsymbol{M_R}\begin{bmatrix}\boldsymbol{\xi}\\1\end{bmatrix}\geq\left(\left(-\mathbf{1}^T\boldsymbol{\xi}\right)^+-\delta\right)^+, \forall\boldsymbol{\xi}\in R^n \tag{A.3}$$

The claim follows.

TABLE IV
PARAMETERS OF THE WIND POWER

t	**1**	**2**	**3**	**4**	**5**	**6**
$P^f_{W,1}$	125.0	125.0	137.5	137.5	150.0	150.0
$\mu_{W,1}$	-0.2500	-0.2500	-0.2635	-0.2592	-0.2750	-0.2662
$\sigma^2_{W,1}$	50.00	50.80	53.35	54.50	57.25	58.60
$P^f_{W,2}$	100. 0	100. 0	110. 0	110. 0	120. 0	120. 0
$\mu_{W,2}$	-0.0040	-0.0040	-0.0042	-0.0041	-0.0044	-0.0043
$\sigma^2_{W,2}$	60.00	60.96	64.02	65.40	68.70	70.32
$P^f_{W,3}$	120.0	120.0	132.0	132.0	144.0	144.0
$\mu_{W,3}$	0.0200	0.0200	0.0211	0.0207	0.0220	0.0213
$\sigma^2_{W,3}$	20.00	20.32	21.34	21.80	22.90	23.44
t	**7**	**8**	**9**	**10**	**11**	**12**
$P^f_{W,1}$	137.5	137.5	125.0	125.0	112.5	112.5
$\mu_{W,1}$	-0.2840	-0.2717	-0.2933	-0.2770	-0.3040	-0.2835
$\sigma^2_{W,1}$	61.45	62.85	65.95	67.45	70.70	72.35
$P^f_{W,2}$	110. 0	110.0	100.0	100.0	90.0	90.0
$\mu_{W,2}$	-0.0045	-0.0043	-0.0047	-0.0044	-0.0049	-0.0045
$\sigma^2_{W,2}$	73.74	75.42	79.14	80.94	84.84	86.82
$P^f_{W,3}$	132.0	132.0	120.0	120.0	108.0	108.0
$\mu_{W,3}$	0.0227	0.0217	0.0235	0.0222	0.0243	0.0227
$\sigma^2_{W,3}$	24.58	25.14	26.38	26.98	28.28	28.94
t	**13**	**14**	**15**	**16**	**17**	**18**
$P^f_{W,1}$	100.0	100.0	87.5	87.5	75.0	75.0
$\mu_{W,1}$	-0.3160	-0.2913	-0.3300	-0.3003	-0.2527	-0.2690
$\sigma^2_{W,1}$	75.75	77.50	80.75	82.20	86.90	94.95
$P^f_{W,2}$	80.0	80.0	70.0	70.0	60.0	60.0
$\mu_{W,2}$	-0.0051	-0.0047	-0.0053	-0.0048	-0.0040	-0.0043
$\sigma^2_{W,2}$	90.90	93.00	96.90	98.64	104.28	113.94
$P^f_{W,3}$	96.0	96.0	84.0	84.0	72.0	72.0
$\mu_{W,3}$	0.0253	0.0233	0.0264	0.0240	0.0202	0.0215
$\sigma^2_{W,3}$	30.30	31.00	32.30	32.88	34.76	37.98
t	**19**	**20**	**21**	**22**	**23**	**24**
$P^f_{W,1}$	62.5	62.5	62.5	62.5	62.5	62.5
$\mu_{W,1}$	-0.2895	-0.3113	-0.3247	-0.3377	-0.3565	-0.3750
$\sigma^2_{W,1}$	103.00	111.35	121.15	131.70	140.65	150.00
$P^f_{W,2}$	50.0	50.0	50.0	50.0	50.0	50.0
$\mu_{W,2}$	-0.0046	-0.0050	-0.0052	-0.0054	-0.0057	-0.0060
$\sigma^2_{W,2}$	123.60	133.62	145.38	158.04	168.78	180.00
$P^f_{W,3}$	60.0	60.0	60.0	60.0	60.0	60.0
$\mu_{W,3}$	0.0232	0.0249	0.0260	0.0270	0.0285	0.0300
$\sigma^2_{W,3}$	41.20	44.54	48.46	52.68	56.26	60.00

* $P^f_{W,i}$ and $\mu_{W,i}, i=1,2,3$ are in MW, $\sigma^2_{W,i}, i=1,2,3$ are in MW^2.

Appendix B

Proposition: $P_{WC}(\boldsymbol{x_t})=\mathop{sup}\limits_{\phi\in\Phi(\mu,\Gamma)}\Pr\left(\bigcup\limits_{k=1}^{N_L+2N_{RT}}\{[\boldsymbol{F_k}(\boldsymbol{x_t})\boldsymbol{z}]^2\geq\gamma_k^2\}\right)$ equals to the objective value of the following problem

$$\begin{aligned} P_{WC}(x_t) = & \underset{M=M^T \in R^{(n+1)\times(n+1)}}{inf} Trace(\boldsymbol{QM}) \\ s.t. \quad & \boldsymbol{M} \geq 0, \\ & \boldsymbol{z^T M z} \geq 1, \forall \boldsymbol{z} : [F_k(\boldsymbol{x_t})\boldsymbol{z}]^2 \geq \gamma_k^2, \\ & k = 1, \ldots, N_L + 2N_{RT} \end{aligned}$$

Proof [29]: Define the indicator function of the union set $S = \overset{N_L+2N_{RT}}{\underset{k=1}{\cup}} \left\{ [\boldsymbol{F_k}(\boldsymbol{x_t})\boldsymbol{z}]^2 \geq \gamma_k^2 \right\}$ as

$$I_S(\boldsymbol{\xi}) = \begin{cases} 1, & \boldsymbol{\xi} \in S \\ 0, & \text{otherwise} \end{cases}.$$

Thus $P_{WC}(\boldsymbol{x_t})$ can be written as

$$P_{WC}(x_t) = \underset{\phi \in \Phi(\mu,\Gamma)}{sup} E[I_S(\boldsymbol{\xi})].$$

By applying similar manipulations as in the proof of Appendix A, and defining $\boldsymbol{z} = \begin{bmatrix} \boldsymbol{\xi}^T & 1 \end{bmatrix}^T$, $P_{WC}(\boldsymbol{x_t})$ can be equivalently expressed as

$$\begin{aligned} & \inf_{\boldsymbol{M}=\boldsymbol{M^T} \in R^{(n+1)\times(n+1)}} Trace(\boldsymbol{QM}) \\ & s.t. \quad \boldsymbol{z}^T \boldsymbol{M z} \geq I_S(\boldsymbol{\xi}), \forall \boldsymbol{\xi} \in R^n \end{aligned} \tag{B.1}$$

The constraint in (B.1) can be expanded as

$$\begin{cases} \boldsymbol{z^T M z} \geq 0, & \forall \boldsymbol{\xi} \in R^n \\ \boldsymbol{z^T M z} \geq 1, & \forall z : [F_k(\boldsymbol{x_t})\boldsymbol{z}]^2 \geq \gamma_k^2, \\ & k = 1, \ldots, N_L + 2N_{RT} \end{cases} \tag{B.2}$$

where the first constraint is equivalent to $\boldsymbol{M} \geq 0$.

Thus the claim follows.

Appendix C

The forecasted value, mean and variance of the wind power output at each time period are listed in Table IV, where $P_{W,i}^f, i = 1, 2, 3$ is the forecasted value of the wind power at the ith wind farm, $\mu_{W,i}, i = 1, 2, 3$ and $\sigma_{W,i}^2, i = 1, 2, 3$ are the mean and variance, respectively.

References

[1] N. Menemenlis, M. Huneault, and A. Robitaille, "Computation of dynamic operating balancing reserve for wind power integration for the time-horizon 1-48 hours," *IEEE Trans. Sustain. Energy*, vol. 3, no. 4, pp. 692–702, Oct. 2012.

[2] M. A. Ortega-Vazquez and D. S. Kirschen, "Estimating the spinning reserve requirements in systems with significant wind power generation penetration," *IEEE Trans. Power Syst.*, vol. 24, no. 1, pp. 114–124, Feb. 2009.

[3] J. M. Morales, A. J. Conejo, and J. Perez-Ruiz, "Economic valuation of reserves in power systems with high penetration of wind power," *IEEE Trans. Power Syst.*, vol. 24, no. 2, pp. 900–910, May 2009.

[4] G. Zhang, W. Wu, and B. Zhang, "Optimization of operation reserve coordination considering wind power integration," *Autom. Electr. Power Syst.*, vol. 35, pp. 15–19, 2011 (in Chinese).

[5] Z. Xue, G. Li, and M. Zhou, "Credibility theory applied for estimating operating reserve considering wind power uncertainty," in *Proc. IEEE Trondheim PowerTech*, Trondheim, Norway, Jun. 19–23, 2011, pp. 1–8.

[6] N. G. Paterakis, O. Erdinc, A. G. Bakirtzis, and J. P. S. Catalao, "Load-following reserves procurement considering flexible demand-side resources under high wind power penetration," *IEEE Trans. Power Syst.*, vol. 30, no. 3, pp. 1337–1350, May 2015.

[7] H. Holttinen *et al.*, "Methodologies to determine operating reserves due to increased wind power," *IEEE Trans. Sustain. Energy*, vol. 3, no. 4, pp. 713–723, Oct. 2012.

[8] F. Bouffard and F. D. Galiana, "Stochastic security for operations planning with significant wind power generation," *IEEE Trans. Power Syst.*, vol. 23, no. 2, pp. 306–316, May. 2008.

[9] T. Wu, Q. Yang, Z. Bao, and W. Yan, "Coordinated energy dispatching in microgrid with wind power generation and plug-in electric vehicles," *IEEE Trans. Smart Grid*, vol. 4, no. 3, pp. 1453–1463, Sep. 2013.

[10] D. Villanueva, J. L. Pazos, and A. Feijoo, "Probabilistic load flow including wind power generation," *IEEE Trans. Power Syst.*, vol. 26, no. 3, pp. 1659–1667, Aug. 2011.

[11] Y. Yuan, J. Zhou, P. Ju, and J. Feuchtwang, "Probabilistic load flow computation of a power system containing wind farms using the method of combined cumulants and Gram–Charlier expansion," *IET Renew. Power Gen.*, vol. 5, pp. 448–454, Nov. 2011.

[12] S. Bofinger, A. Luig, and H. G. Beyer, "Qualification of wind power forecasts," in *Proc. Global Wind Power Conf.*, Paris, France, Apr. 2002.

[13] M. H. Albadi and E. F. El-Saadany, "Comparative study on impacts of wind profiles on thermal units scheduling costs," *IET Renew. Power Gen.*, vol. 5, pp. 26–35, Jan. 2011.

[14] H. Bludszuweit, J. A. Dominguez-Navarro, and A. Llombart, "Statistical analysis of wind power forecast error," *IEEE Trans. Power Syst.*, vol. 23, no. 3, pp. 983–991, Aug. 2008.

[15] S. Tewari, C. J. Geyer, and N. Mohan, "A statistical model for wind power forecast error and its application to the estimation of penalties in liberalized markets," *IEEE Trans. Power Syst.*, vol. 26, no. 4, pp. 2031–2039, Nov. 2011.

[16] A. Luig, S. Bofinger, and H. G. Beyer, "Analysis of confidence intervals for the prediction of regional wind power output," in *Proc. European Wind Energy Assoc. Conf. (EWEC'01)*, Jul. 2001, pp. 725–728.

[17] A. Fabbri, T. G. S. Roman, J. R. Abbad, and V. M. Quezada, "Assessment of the cost associated with wind generation prediction errors in a liberalized electricity market," *IEEE Trans. Power Syst.*, vol. 20, no. 3, pp. 1440–1446, Aug. 2005.

[18] J. Wu, B. Zhang, H. Li, Z. Li, Y. Chen, and X. Miao, "Statistical distribution for wind power forecast error and its application to determine optimal size of energy storage system," *Int. J. Electr. Power*, vol. 55, pp. 100–107, Feb. 2014.

[19] B. Hodge and M. Milligan, "Wind power forecasting error distributions over multiple timescales," in *Proc. IEEE Power Energy Soc. Gen. Meeting (PES'11)*, Jul. 2011, pp. 1–8.

[20] K. Bruninx and E. Delarue, "A statistical description of the error on wind power forecasts for probabilistic reserve sizing," *IEEE Trans. Sustain. Energy*, vol. 5, no. 3, pp. 995–1002, Jul. 2014.

[21] I. Pólik and T. Terlaky, "A survey of the S-lemma," *SIAM Rev.*, vol. 49, pp. 371–418, Jul. 2007.

[22] S. Boyd and L. Vandenberghe, *Convex Optimization*. Cambridge, U.K.: Cambridge Univ. Press, 2004.

[23] Q. Bian, H. Xin, Z. Wang, D. Gan, and K. P. Wong, "Distributionally robust solution to the reserve scheduling problem with partial information of wind power," *IEEE Trans. Power Syst.*, vol. 30, no. 5, pp. 2822–2823, Sep. 2015.

[24] R. T. Rockafellar and S. Uryasev, "Conditional value-at-risk for general loss distributions," *J. Banking Finance*, May. 2002.

[25] P. Jorion, *Value at Risk: The New Benchmark for Managing Financial Risk*, 3rd ed.. New York, NY, USA: McGraw-Hill, 2006.

[26] T. Ackermann, *Wind Power in Power Systems*. Hoboken, NJ, USA: Wiley, 2005.

[27] W. Wu, B. Zhang, J. Chen, and T. Zhen, "Multiple time-scale coordinated power control system to accommodate significant wind power penetration and its real application," in *Proc. IEEE Power Energy Syst. Gen. Meeting (PES'12)*, San Diego, CA, USA, Jul. 22–26, 2012, pp. 1–6.

[28] S. Zymler, D. Kuhn, and B. Rustem, "Distributionally robust joint chance constraints with second-order moment information," *Math. Program.*, vol. 137, pp. 167–198, Feb. 2013.

[29] G. Calafiore, U. Topcu, and L. El Ghaoui, "Parameter estimation with expected and residual-at-risk criteria," *Syst. Control Lett.*, vol. 58, pp. 39–46, Jan. 2009.

[30] J. Korski, F. Pfeuffer, and K. Klamroth, "Biconvex sets and optimization with biconvex functions: A survey and extensions," *Math. Methods Oper. Res.*, vol. 66, pp. 373–407, 2007.

[31] M. A. Pai, *Energy Function Analysis for Power System Stability*. Norwell, MA, USA: Kluwer, 1989.

[32] J. Löfberg, "YALMIP: A toolbox for modeling and optimization in MATLAB," in *Proc. IEEE Int.Symp. Comput. Aided Control Syst. Design*, Sep. 2004, pp. 284–289.

[33] V. Torczon, "On the convergence of pattern search algorithms," *SIAM J. Optim.*, vol. 7, pp. 1–25, 1997.

Zhen Wang (M'11) received the B.Eng. degree from Xi'an Jiaotong University, Xi'an, China, the M.Eng. degree from Zhejiang University, Zhejiang, China, and the Ph.D. degree from Hong Kong Polytechnic University, Hong Kong, in 1998, 2001, and 2009, respectively. He is currently an Associate Professor with the Department of Electrical Engineering, Zhejiang University. He was a Visiting Scholar at the University of Western Australia, Crawley, W.A., Australia, from February 2014 to August 2014. His research interests include power system stability and control, computational intelligence, and renewable energy. He was the recipient of 2014 Endeavour Research Fellowship sponsored by Australia Government

Qiaoyan Bian (S'13) received the B.Eng. and the Ph.D. degrees in electrical engineering from Zhejiang University, Zhejiang, China, in 2008 and 2015, respectively. From March 2010 to April 2013, she was a training jointly Doctoral Student with the Electrical and Computer Engineering Department, University of Oklahoma, Norman, OK, USA. Her research interests include power system operation and planning, renewable energy integration and ancillary services.

Huanhai Xin (M'14) received the Ph.D. degree in electrical engineering from Zhejiang University, Zhejiang, China, in 2007. He is currently a Professor with the Department of Electrical Engineering, Zhejiang University. From June 2009 to July 2010, he was a Postdoctoral Fellow with the Electrical Engineering and Computer Science Department, the University of Central Florida, Orlando, FL, USA. His research interests include power system stability analysis and control, and renewable energy integration. He was the recipient of the best paper prize in the IEEE PES General Meeting, 2013.

Deqiang Gan (M'96–SM'01) received the Ph.D. degree in electrical engineering from Xi'an Jiaotong University, X'ian, China, in 1994. He has been with the Faculty of Zhejiang University since 2002. His employment experience includes ISO New England, Inc., Ibaraki University, University of Central Florida, and Cornell University. His research interests include power system stability and market operations. He is currently serving as an Editor for the INTERNATIONAL TRANSACTIONS ON ELECTRICAL ENERGY SYSTEMS.